This is a repository copy of *Analytical magnetic field analysis of Halhach magnetized permanent-magnet machines* .

White Rose Research Online URL for this paper:
http://eprints.whiterose.ac.uk/867/

eprints@whiterose.ac.uk
https://eprints.whiterose.ac.uk/

Analytical Magnetic Field Analysis of Halbach Magnetized Permanent-Magnet Machines

Z. P. Xia, Z. Q. Zhu, *Senior Member, IEEE*, and D. Howe

Abstract—We develop analytical models for predicting the magnetic field distribution in Halbach magnetized machines. They are formulated in polar coordinates and account for the relative recoil permeability of the magnets. They are applicable to both internal and external rotor permanent-magnet machines with either an iron-cored or air-cored stator and/or rotor. We compare predicted results with those obtained by finite-element analyses and measurements. We show that the air-gap flux density varies significantly with the pole number and that an optimal combination of the magnet thickness and the pole number exists for maximum air-gap flux density, while the back iron can enhance the air-gap field and electromagnetic torque when the radial thickness of the magnet is small.

Index Terms—Electrical machines, magnetic field, permanent magnet.

I. INTRODUCTION

HALBACH magnetized permanent-magnet machines offer several potentially attractive features [1]. First, they have an essentially sinusoidal air-gap field distribution. Hence, their induced electromotive force (EMF) waveform is inherently sinusoidal and the cogging torque may be negligible, without resorting to skew or a distributed stator winding. Second, since the magnetic field in Halbach magnetized machines is essentially self-shielding, the rotor back iron is not essential. Thus, either an iron-cored or an air-cored rotor may be used. However, as will be shown in the paper, some benefits can be derived by employing the rotor back iron, in terms of reducing the volume of magnet material required to achieve a given level of performance.

The concept of Halbach magnetization was originally proposed by Halbach [2], although initially electrical machines employed segmented magnets which only approximated the Halbach magnetization [3], [4]. However, high-performance bonded NdFeB magnets have facilitated the manufacture of near ideal multipole magnetized Halbach ring magnets. For example, an isotropic NdFeB Halbach magnetized ring magnet was produced using a specially designed magnetizing fixture in [5], while an anisotropic NdFeB Halbach magnetized ring magnet was produced by employing a combination of a magnet powder alignment system and a custom magnetizing fixture in [6] and [7].

The magnetic field analyses for segmented magnet Halbach magnetized machines were derived in [1]–[3]. This paper presents analytical models for predicting the magnetic field distribution in air-cored and iron-cored internal and external field Halbach
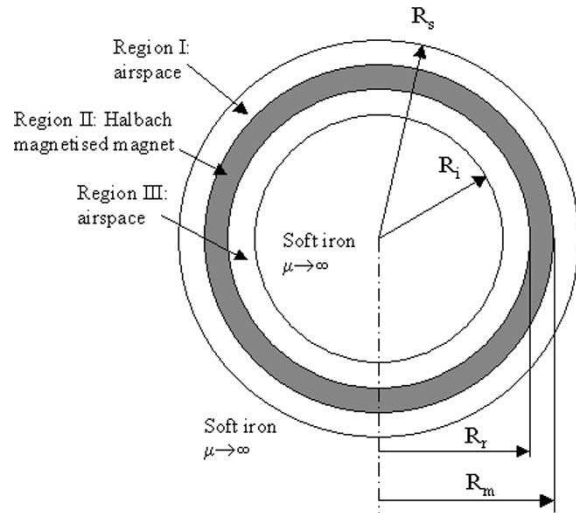
Fig. 1. General analytical model for field calculation in a Halbach magnetized magnet machine.

machines which are equipped with ideal Halbach magnetized magnets. They are formulated in polar coordinates, and account for the relative recoil permeability of the magnet. The influence of back iron and the optimal combination of magnet thickness and pole number for maximum air-gap flux density are also investigated. Analytically predicted results are compared with those obtained by finite-element analysis and measurements.

II. ANALYTICAL MODELS FOR PREDICTING MAGNETIC FIELD

The analytical model shown in Fig. 1 is divided into three annular regions, in which region II is the Halbach magnetized magnet, and the other regions are air spaces. As will be seen later in the paper, this is necessary in order to make the solutions generally applicable to air-cored and iron-cored machines. In Fig. 1, R_s, R_m, R_r, and R_i are the outer bore radius, the outer and inner radii of the magnet, and the inner bore radius, respectively. The winding can be inserted into either region I or region III, depending on whether the machine is an internal field or external field Halbach magnetized magnet machine, while one of the air gaps may be reduced to zero for an iron-cored machine, or be increased for an air-cored machine. In order to obtain an analytical solution for the field distribution produced in a multipole Halbach magnetized magnet machine, the following assumptions are made.

1) The magnet is oriented according to the Halbach magnetization and is fully magnetized in the direction of magnetization.
2) The effect of the finite axial length is neglected, i.e., an infinitely long machine is considered.
3) The back iron is infinitely permeable.

The field vectors $\vec{B}$ and $\vec{H}$ are coupled by

$$\vec{B} = \mu_0 \vec{H} \quad \text{in the air space} \tag{1}$$

$$\vec{B} = \mu_0 \mu_r \vec{H} + \mu_0 \vec{M} \quad \text{in the permanent magnet} \tag{2}$$

where μ_0 is the permeability of free space and μ_r is the relative recoil permeability of the magnet.

For a Halbach magnetized magnet machine, the magnetization distribution $\vec{M}$ varies sinusoidally. In polar coordinates, it is given by

$$\vec{M} = M_r \vec{e}_r + M_\theta \vec{e}_\theta = M \cos p\theta \, \vec{e}_r \mp M \sin p\theta \, \vec{e}_\theta \tag{3}$$

where $-$ is for an internal rotor machine (external field), $+$ is for an external rotor machine (internal field), $\vec{e}_r$ and $\vec{e}_\theta$ are the unit vectors in the radial and circumferential directions, respectively, p is the number of pole pairs, $M = (B_r/\mu_0)$ is the amplitude of magnetization, and B_r is the remanence of the magnet.

The magnetic field produced by a Halbach magnetized magnet machine can be described by the scalar magnetic potential φ

$$\nabla^2 \varphi_{\mathrm{I}} = \frac{\partial^2 \varphi_{\mathrm{I}}}{\partial r^2} + \frac{1}{r}\frac{\partial \varphi_{\mathrm{I}}}{\partial r} + \frac{1}{r^2}\frac{\partial^2 \varphi_{\mathrm{I}}}{\partial \theta^2} = 0$$
$$\text{in region I (air space)}, \quad R_m < r < R_s \tag{4}$$

$$\nabla^2 \varphi_{\mathrm{II}} = \frac{\partial^2 \varphi_{\mathrm{II}}}{\partial r^2} + \frac{1}{r}\frac{\partial \varphi_{\mathrm{II}}}{\partial r} + \frac{1}{r^2}\frac{\partial^2 \varphi_{\mathrm{II}}}{\partial \theta^2} = \frac{\mathrm{div}\vec{M}}{\mu_r}$$
$$\text{in region II (magnet)}, \quad R_r < r < R_m \tag{5}$$

$$\nabla^2 \varphi_{\mathrm{III}} = \frac{\partial^2 \varphi_{\mathrm{III}}}{\partial r^2} + \frac{1}{r}\frac{\partial \varphi_{\mathrm{III}}}{\partial r} + \frac{1}{r^2}\frac{\partial^2 \varphi_{\mathrm{III}}}{\partial \theta^2} = 0$$
$$\text{in region III (air space)}, \quad R_i < r < R_r \tag{6}$$

where $\mathrm{div}\vec{M} = (M_r/r) + (\partial M_r/\partial r) + (1/r)(\partial M_\theta/\partial \theta) = (1 \mp p)(M/r)\cos p\theta$ and where φ_{I}, φ_{II}, and φ_{III} are related to the radial and circumferential components of $\vec{H}$ by

$$\vec{H} = -\,\mathrm{grad}\,\varphi \tag{7a}$$

$$H_r = -\frac{\partial \varphi}{\partial r} \quad \text{and} \quad H_\theta = -\frac{1}{r}\frac{\partial \varphi}{\partial \theta}. \tag{7b}$$

For both internal and external rotor machines, the general solutions of (4)–(6) are

$$\varphi_{\mathrm{I}}(r,\theta) = (C_1 r^p + C_2 r^{-p})\cos p\theta \tag{8}$$

$$\varphi_{\mathrm{II}}(r,\theta) = (C_3 r^p + C_4 r^{-p})\cos p\theta + \frac{B_r}{\mu_0 \mu_r}\frac{r}{1 \pm p}\cos p\theta \tag{9}$$

$$\varphi_{\mathrm{III}}(r,\theta) = (C_5 r^p + C_6 r^{-p})\cos p\theta. \tag{10}$$

Here, it should be noted that $+$ is for internal rotor machine, and $-$ is for external rotor machine.

The boundary conditions to be satisfied are

$$H_{\theta\mathrm{I}}|_{r=R_s} = 0 \tag{11}$$

$$B_{r\mathrm{I}} = B_{r\mathrm{II}}|_{r=R_m}, \quad H_{\theta\mathrm{I}} = H_{\theta\mathrm{II}}|_{r=R_m} \tag{12}$$

$$B_{r\mathrm{II}} = B_{r\mathrm{III}}|_{r=R_r}, \quad H_{\theta\mathrm{II}} = H_{\theta\mathrm{III}}|_{r=R_r} \tag{13}$$

$$H_{\theta\mathrm{III}}|_{r=R_i} = 0. \tag{14}$$

The expression of H and B for the three regions are given by

$$H_{\mathrm{I}r} = -\frac{\partial \varphi_{\mathrm{I}}}{\partial r} = -p(C_1 r^{p-1} - C_2 r^{-p-1})\cos p\theta \tag{15}$$

$$B_{\mathrm{I}r} = \mu_0 H_{\mathrm{I}r} = \mu_0 p(-C_1 r^{p-1} + C_2 r^{-p-1})\cos p\theta \tag{16}$$

$$H_{\mathrm{I}\theta} = -\frac{1}{r}\frac{\partial \varphi_{\mathrm{I}}}{\partial \theta} = p(C_1 r^{p-1}) + C_2 r^{-p-1})\sin p\theta \tag{17}$$

$$B_{\mathrm{I}\theta} = \mu_o H_{\mathrm{I}\theta} = \mu_o p(C_1 r^{p-1} + C_2 r^{-p-1})\sin p\theta \tag{18}$$

$$H_{\mathrm{II}r} = -\frac{\partial \varphi_{\mathrm{II}}}{\partial r} = (-pC_3 r^{p-1} + pC_4 r^{-p-1})\cos p\theta$$
$$- \frac{B_r}{\mu_o \mu_r (1 \pm p)}\cos p\theta \tag{19}$$

$$\begin{aligned} B_{\mathrm{II}r} &= \mu_0 \mu_r H_{\mathrm{II}r} + \mu_0 M_r \\ &= \mu_0 \mu_r p(-C_3 r^{p-1} + C_4 r^{-p-1})\cos p\theta \\ &\pm \frac{p}{p \pm 1} B_r \cos p\theta \end{aligned} \tag{20}$$

$$\begin{aligned} H_{\mathrm{II}\theta} &= -\frac{1}{r}\frac{\partial \varphi_{\mathrm{II}}}{\partial \theta} = p(C_3 r^{p-1} + C_4 r^{-p-1})\sin p\theta \\ &+ \frac{B_r}{\mu_0 \mu_r}\frac{p}{1 \pm p}\sin p\theta \end{aligned} \tag{21}$$

$$\begin{aligned} B_{\mathrm{II}\theta} &= \mu_0 \mu_r H_{\mathrm{II}\theta} + \mu_0 M_\theta = \mu_0 \mu_r p(C_3 r^{p-1} + C_4 r^{-p-1})\sin p\theta \\ &\mp \frac{B_r}{1 \pm p}\sin p\theta \end{aligned} \tag{22}$$

$$H_{\mathrm{III}r} = -\frac{\partial \varphi_{\mathrm{III}}}{\partial r} = p(-C_5 r^{p-1} + C_6 r^{-p-1})\cos p\theta \tag{23}$$

$$B_{\mathrm{III}r} = \mu_0 H_{\mathrm{III}r} = \mu_0 p(-C_5 r^{p-1} + C_6 r^{-p-1})\cos p\theta \tag{24}$$

$$H_{\mathrm{III}\theta} = -\frac{1}{r}\frac{\partial \varphi_{\mathrm{III}}}{\partial \theta} = p(C_5 r^{p-1} + C_6 r^{-p-1})\sin p\theta \tag{25}$$

$$B_{\mathrm{III}\theta} = \mu_0 H_{\mathrm{III}\theta} = \mu_0 p(C_5 r^{p-1} + C_6 r^{-p-1})\sin p\theta. \tag{26}$$

Application of the boundary conditions (11)–(14) to the above (15)–(26) gives

$$C_0 = R_s^{2p} D_0 \tag{27}$$

$$\begin{aligned} D_0 = &\left[(1 - \mu_r)\left(\frac{R_r}{R_m}\right)^{2p} + (1 + \mu_r)\left(\frac{R_i}{R_m}\right)^{2p}\right] \\ &\times \left[(1 - \mu_r) + (1 + \mu_r)\left(\frac{R_m}{R_s}\right)^{2p}\right] \\ &- \left[(1 + \mu_r) + (1 - \mu_r)\left(\frac{R_m}{R_s}\right)^{2p}\right] \\ &\times \left[(1 + \mu_r) + (1 - \mu_r)\left(\frac{R_i}{R_r}\right)^{2p}\right]. \end{aligned} \tag{28}$$

For an internal rotor machine

$$C_1 = \frac{D_1}{C_0}\frac{1}{p\mu_0}R_m^{p+1}$$

$$C_2 = -C_1 R_s^{2p}$$

$$C_3 = \frac{(1 + \mu_r) + (1 - \mu_r)\left(\frac{R_s}{R_m}\right)^{2p}}{2\mu_r}C_1$$

$$\begin{aligned} C_4 = &\frac{(1 - \mu_r)R_m^{2p} + (1 + \mu_r)R_s^{2p}}{-2\mu_r}C_1 \\ &- \frac{\frac{B_r}{\mu_o}}{\mu_r(1 + p)}R_m^{p+1} \end{aligned}$$

$$C_5 = \frac{D_2}{C_0}\frac{1}{p\mu_0}R_m^{p+1}\left(\frac{R_s}{R_m}\right)^{2p}$$

$$C_6 = -C_5 R_i^{2p} \tag{29}$$

$$D_1 = \frac{2B_r p}{1+p}\left[(1+\mu_r)+(1-\mu_r)\left(\frac{R_i}{R_r}\right)^{2p}\right]$$
$$\times \left[1-\left(\frac{R_r}{R_m}\right)^{p+1}\right] \tag{30}$$

$$D_2 = \frac{2B_r p}{1+p}\left[(1-\mu_r)+(1+\mu_r)\left(\frac{R_m}{R_s}\right)^{2p}\right]$$
$$\times \left[1-\left(\frac{R_r}{R_m}\right)^{p+1}\right] \tag{31}$$

and similarly for an external rotor machine

$$C_1 = \frac{D_1}{C_0}\frac{1}{p\mu_0}R_r{}^{2p}R_m{}^{1-p}$$
$$C_2 = -C_1 R_s{}^{2p}$$
$$C_3 = \frac{(1+\mu_r)+(1-\mu_r)\left(\frac{R_s}{R_m}\right)^{2p}}{2\mu_r}C_1$$
$$\quad - \frac{\frac{B_r}{\mu_o}}{\mu_r(1-p)}R_m{}^{1-p}$$
$$C_4 = \frac{(1-\mu_r)R_m{}^{2p}+(1+\mu_r)R_s{}^{2p}}{-2\mu_r}C_1$$
$$C_5 = \frac{D_2}{C_0}\frac{1}{p\mu_0}R_m{}^{1-p}$$
$$C_6 = -C_5 R_I{}^{2p} \tag{32}$$
$$D_1 = \frac{2B_r p}{1-p}\left[(1-\mu_r)+(1+\mu_r)\left(\frac{R_i}{R_r}\right)^{2p}\right]$$
$$\times \left[1-\left(\frac{R_r}{R_m}\right)^{1-p}\right] \tag{33}$$

$$D_2 = \frac{2B_r p}{1-p}\left[(1+\mu_r)+(1-\mu_r)\left(\frac{R_m}{R_s}\right)^{2p}\right]$$
$$\times \left[1-\left(\frac{R_r}{R_m}\right)^{1-p}\right]. \tag{34}$$

Therefore, the flux density distribution in regions I and III of the internal rotor machine can be deduced from (16), (18), (24), and (26)

$$B_{\mathrm{I}r} = -\frac{D_1}{D_0}\left[\left(\frac{r}{R_s}\right)^{p-1}\left(\frac{R_m}{R_s}\right)^{p+1}+\left(\frac{R_m}{r}\right)^{p+1}\right]\cos p\theta \tag{35}$$

$$B_{\mathrm{I}\theta} = \frac{D_1}{D_0}\left[\left(\frac{r}{R_s}\right)^{p-1}\left(\frac{R_m}{R_s}\right)^{p+1}-\left(\frac{R_m}{r}\right)^{p+1}\right]\sin p\theta \tag{36}$$

$$B_{\mathrm{III}r} = -\frac{D_2}{D_0}\left[\left(\frac{r}{R_m}\right)^{p-1}+\left(\frac{R_i}{R_m}\right)^{p-1}\left(\frac{R_i}{r}\right)^{p+1}\right]\cos p\theta \tag{37}$$

$$B_{\mathrm{III}\theta} = \frac{D_2}{D_0}\left[\left(\frac{r}{R_m}\right)^{p-1}-\left(\frac{R_i}{R_m}\right)^{p-1}\left(\frac{R_i}{r}\right)^{p+1}\right]\sin p\theta. \tag{38}$$

If $\mu_r = 1$, the above expressions can be simplified significantly, to

$$B_{\mathrm{I}r} = B_r\frac{p}{p+1}\frac{1-\left(\frac{R_r}{R_m}\right)^{p+1}}{1-\left(\frac{R_i}{R_s}\right)^{2p}}$$
$$\times \left[\left(\frac{r}{R_s}\right)^{p-1}\left(\frac{R_m}{R_s}\right)^{p+1}+\left(\frac{R_m}{r}\right)^{p+1}\right]\cos p\theta \tag{39}$$

$$B_{\mathrm{I}\theta} = -B_r\frac{p}{p+1}\frac{1-\left(\frac{R_r}{R_m}\right)^{p+1}}{1-\left(\frac{R_i}{R_s}\right)^{2p}}$$
$$\times \left[\left(\frac{r}{R_s}\right)^{p-1}\left(\frac{R_m}{R_s}\right)^{p+1}-\left(\frac{R_m}{r}\right)^{p+1}\right]\sin p\theta \tag{40}$$

$$B_{\mathrm{III}r} = B_r\frac{p}{p+1}\frac{1-\left(\frac{R_r}{R_m}\right)^{p+1}}{1-\left(\frac{R_i}{R_s}\right)^{2p}}\left(\frac{R_m}{R_s}\right)^{2p}$$
$$\times \left[\left(\frac{r}{R_m}\right)^{p-1}+\left(\frac{R_i}{R_m}\right)^{p-1}\left(\frac{R_i}{r}\right)^{p+1}\right]\cos p\theta \tag{41}$$

$$B_{\mathrm{III}\theta} = -B_r\frac{p}{p+1}\frac{1-\left(\frac{R_r}{R_m}\right)^{p+1}}{1-\left(\frac{R_i}{R_s}\right)^{2p}}\left(\frac{R_m}{R_s}\right)^{2p}$$
$$\times \left[\left(\frac{r}{R_m}\right)^{p-1}-\left(\frac{R_i}{R_m}\right)^{p-1}\left(\frac{R_i}{r}\right)^{p+1}\right]\sin p\theta. \tag{42}$$

Similarly, the flux density distribution in regions I and III of an external rotor machine is

$$B_{\mathrm{I}r} = -\frac{D_1}{D_0}\left[\left(\frac{R_r}{R_s}\right)^{2p}\left(\frac{r}{R_m}\right)^{p-1}+\left(\frac{R_r}{R_m}\right)^{p-1}\left(\frac{R_r}{r}\right)^{p+1}\right]\cos p\theta \tag{43}$$

$$B_{\mathrm{I}\theta} = \frac{D_1}{D_0}\left[\left(\frac{R_r}{R_s}\right)^{2p}\left(\frac{r}{R_m}\right)^{p-1}-\left(\frac{R_r}{R_m}\right)^{p-1}\left(\frac{R_r}{r}\right)^{p+1}\right]\sin p\theta \tag{44}$$

$$B_{\mathrm{III}r} = -\frac{D_2}{D_0}\left[\left(\frac{r}{R_m}\right)^{p-1}+\left(\frac{R_i}{R_m}\right)^{p-1}\left(\frac{R_i}{r}\right)^{p+1}\right]\cos p\theta \tag{45}$$

$$B_{\mathrm{III}\theta} = \frac{D_2}{D_0}\left[\left(\frac{r}{R_m}\right)^{p-1}-\left(\frac{R_i}{R_m}\right)^{p-1}\left(\frac{R_i}{r}\right)^{p+1}\right]\sin p\theta. \tag{46}$$

Again, when $\mu_r = 1$, the foregoing equations are simplified to

$$B_{\mathrm{I}r} = B_r\frac{p}{1-p}\frac{1-\left(\frac{R_r}{R_m}\right)^{1-p}}{1-\left(\frac{R_i}{R_s}\right)^{2p}}\left(\frac{R_i}{R_r}\right)^{2p}$$
$$\times \left[\left(\frac{R_r}{R_s}\right)^{2p}\left(\frac{r}{R_m}\right)^{p-1}+\left(\frac{R_r}{R_m}\right)^{p-1}\left(\frac{R_r}{r}\right)^{p+1}\right]\cos p\theta \tag{47}$$

$$B_{\mathrm{I}\theta} = -B_r \frac{p}{1-p} \frac{1-\left(\frac{R_r}{R_m}\right)^{1-p}}{1-\left(\frac{R_i}{R_s}\right)^{2p}} \left(\frac{R_i}{R_r}\right)^{2p}$$
$$\times \left[\left(\frac{R_r}{R_s}\right)^{2p}\left(\frac{r}{R_m}\right)^{p-1} - \left(\frac{R_r}{R_m}\right)^{p-1}\left(\frac{R_r}{r}\right)^{p+1}\right] \sin p\theta \tag{48}$$

$$B_{\mathrm{III}r} = B_r \frac{p}{1-p} \frac{1-\left(\frac{R_r}{R_m}\right)^{1-p}}{1-\left(\frac{R_i}{R_s}\right)^{2p}}$$
$$\times \left[\left(\frac{r}{R_m}\right)^{p-1} + \left(\frac{R_i}{R_m}\right)^{p-1}\left(\frac{R_i}{r}\right)^{p+1}\right] \cos p\theta \tag{49}$$

$$B_{\mathrm{III}\theta} = -B_r \frac{p}{1-p} \frac{1-\left(\frac{R_r}{R_m}\right)^{1-p}}{1-\left(\frac{R_i}{R_s}\right)^{2p}}$$
$$\times \left[\left(\frac{r}{R_m}\right)^{p-1} - \left(\frac{R_i}{R_m}\right)^{p-1}\left(\frac{R_i}{r}\right)^{p+1}\right] \sin p\theta. \tag{50}$$

III. ANALYSIS OF MAGNETIC FIELD IN ALTERNATIVE HALBACH MAGNETIZED PERMANENT-MAGNET MACHINES

Three special cases, i.e., iron-cored Halbach machine, air-cored Halbach machine, and Halbach machine in the air space, can be derived from the preceding field solutions. In order to ease the dicussion, they are classified into internal rotor and external rotor machines.

For example, for an internal rotor (external field) machine, the radial and circumferential components of magnetic field in the effective air space (region I) are given as follows:

1) Iron-cored Halbach machine, i.e., $R_i = R_r$

$$B_{\mathrm{I}r} = -\frac{4B_r}{D_0} \frac{p}{1+p} \left[1-\left(\frac{R_r}{R_m}\right)^{p+1}\right]$$
$$\times \left[\left(\frac{r}{R_s}\right)^{p-1}\left(\frac{R_m}{R_s}\right)^{p+1} + \left(\frac{R_m}{r}\right)^{p+1}\right] \cos p\theta \tag{51}$$

$$B_{\mathrm{I}\theta} = \frac{4B_r}{D_0} \frac{p}{1+p} \left[1-\left(\frac{R_r}{R_m}\right)^{p+1}\right]$$
$$\times \left[\left(\frac{r}{R_s}\right)^{p-1}\left(\frac{R_m}{R_s}\right)^{p+1} - \left(\frac{R_m}{r}\right)^{p+1}\right] \sin p\theta \tag{52}$$

$$D_0 = 2\left\{\left(\frac{R_r}{R_m}\right)^{2p}\left[(1-\mu_r)+(1+\mu_r)\left(\frac{R_m}{R_s}\right)^{2p}\right] - \left[(1+\mu_r)+(1-\mu_r)\left(\frac{R_m}{R_s}\right)^{2p}\right]\right\} \tag{53}$$

If $\mu_r = 1$, the equations are simplified to

$$B_{\mathrm{I}r} = B_r \frac{p}{1+p} \frac{1-\left(\frac{R_r}{R_m}\right)^{p+1}}{1-\left(\frac{R_r}{R_s}\right)^{2p}}$$
$$\times \left[\left(\frac{r}{R_s}\right)^{p-1}\left(\frac{R_m}{R_s}\right)^{p+1} + \left(\frac{R_m}{r}\right)^{p+1}\right] \cos p\theta \tag{54}$$

$$B_{\mathrm{I}\theta} = -B_r \frac{p}{1+p} \frac{1-\left(\frac{R_r}{R_m}\right)^{p+1}}{1-\left(\frac{R_r}{R_s}\right)^{2p}}$$
$$\times \left[\left(\frac{r}{R_s}\right)^{p-1}\left(\frac{R_m}{R_s}\right)^{p+1} - \left(\frac{R_m}{r}\right)^{p+1}\right] \sin p\theta \tag{55}$$

2) Air-cored Halbach machine, i.e. $R_i \to 0$

$$B_{\mathrm{I}r} = -\frac{4B_r}{D_0} \frac{p}{1+p} (1+\mu_r)\left[1-\left(\frac{R_r}{R_m}\right)^{p+1}\right]$$
$$\times \left[\left(\frac{r}{R_s}\right)^{p-1}\left(\frac{R_m}{R_s}\right)^{p+1} + \left(\frac{R_m}{r}\right)^{p+1}\right] \cos p\theta \tag{56}$$

$$B_{\mathrm{I}\theta} = \frac{4B_r}{D_0} \frac{p}{1+p} (1+\mu_r)\left[1-\left(\frac{R_r}{R_m}\right)^{p+1}\right]$$
$$\times \left[\left(\frac{r}{R_s}\right)^{p-1}\left(\frac{R_m}{R_s}\right)^{p+1} - \left(\frac{R_m}{r}\right)^{p+1}\right] \sin p\theta \tag{57}$$

$$D_0 = 2\left\{(1-\mu_r)\left(\frac{R_r}{R_m}\right)^{2p}\left[(1-\mu_r)+(1+\mu_r)\left(\frac{R_m}{R_s}\right)^{2p}\right] - (1+\mu_r)\left[(1+\mu_r)+(1-\mu_r)\left(\frac{R_m}{R_s}\right)^{2p}\right]\right\} \tag{58}$$

If $\mu_r = 1$, the equations are simplified to

$$B_{\mathrm{I}r} = B_r \frac{p}{1+p} \left[1-\left(\frac{R_r}{R_m}\right)^{p+1}\right]$$
$$\times \left[\left(\frac{r}{R_s}\right)^{p-1}\left(\frac{R_m}{R_s}\right)^{p+1} + \left(\frac{R_m}{r}\right)^{p+1}\right] \cos p\theta \tag{59}$$

$$B_{\mathrm{I}\theta} = -B_r \frac{p}{1+p} \left[1-\left(\frac{R_r}{R_m}\right)^{p+1}\right]$$
$$\times \left[\left(\frac{r}{R_s}\right)^{p-1}\left(\frac{R_m}{R_s}\right)^{p+1} - \left(\frac{R_m}{r}\right)^{p+1}\right] \sin p\theta \tag{60}$$

3) Halbach machine in air, i.e. $R_i \to 0, R_s \to \infty$

$$B_{\mathrm{I}r} = \frac{-\frac{2B_r p}{1+p}(1+\mu_r)\left[1-\left(\frac{R_r}{R_m}\right)^{p+1}\right]\left(\frac{R_m}{r}\right)^{p+1}}{(1-\mu_r)^2\left(\frac{R_r}{R_m}\right)^{2p} - (1+\mu_r)^2} \cos p\theta \tag{61}$$

$$B_{\mathrm{I}\theta} = \frac{-\frac{2B_r p}{1+p}(1+\mu_r)\left[1-\left(\frac{R_r}{R_m}\right)^{p+1}\right]\left(\frac{R_m}{r}\right)^{p+1}}{(1-\mu_r)^2\left(\frac{R_r}{R_m}\right)^{2p} - (1+\mu_r)^2} \sin p\theta \tag{62}$$

Further, when $\mu_r = 1$, the equations are simplified to

$$B_{\mathrm{I}r} = B_r \frac{p}{p+1} \left[1-\left(\frac{R_r}{R_m}\right)^{p+1}\right]\left(\frac{R_m}{r}\right)^{p+1} \cos p\theta \tag{63}$$

$$B_{\mathrm{I}\theta} = -B_r \frac{p}{p+1} \left[1-\left(\frac{R_r}{R_m}\right)^{p+1}\right]\left(\frac{R_m}{r}\right)^{p+1} \sin p\theta \tag{64}$$

The radial component of air-gap flux density in air-cored and iron-cored internal rotor machines can be expressed in the following unified form, viz.:

$$B_{\text{air gap}} = B_{Ir} = -\frac{4B_r p}{D_0(1+p)}\left[1-\left(\frac{R_r}{R_m}\right)^{p+1}\right]$$

$$\times\left[\left(\frac{r}{R_s}\right)^{p-1}\left(\frac{R_m}{R_s}\right)^{p+1}+\left(\frac{R_m}{r}\right)^{p+1}\right]\cos p\theta \quad (65)$$

$$D_0 = 2\left\{K\left(\frac{R_r}{R_m}\right)^{2p}\left[(1-\mu_r)+(1+\mu_r)\left(\frac{R_m}{R_s}\right)^{2p}\right]\right.$$

$$\left. -\left[(1+\mu_r)+(1-\mu_r)\left(\frac{R_m}{R_s}\right)^{2p}\right]\right\} \quad (66)$$

where $K = 1$ and $(1-\mu_r)/(1+\mu_r)$ for iron-cored and air-cored rotor machines, respectively.

When $\mu_r = 1$, their ratio at the same radius can be expressed as

$$\frac{B_{\text{air gap}}(\text{air-cored})}{B_{\text{air gap}}(\text{iron-cored})} = 1-\left(\frac{R_r}{R_s}\right)^{2p}. \quad (67)$$

Clearly, it depends on the pole number and the ratio of R_r/R_s, or the ratio of R_r/R_m if the air-gap length $(R_s - R_m)$ is fixed.

Similarly, the radial and circumferential components of magnetic field in the effective air space (region III) of an external rotor (internal field) machine are given as follows:

a) Iron-cored Halbach machine, i.e., $R_s = R_m$

$$B_{\text{III}r} = \frac{4B_r}{D_0}\frac{p}{1-p}\left[1-\left(\frac{R_r}{R_m}\right)^{p-1}\right]$$

$$\times\left[1+\left(\frac{R_i}{r}\right)^{2p}\right]\left(\frac{r}{R_r}\right)^{p-1}\cos p\theta \quad (68)$$

$$B_{\text{III}\theta} = -\frac{4B_r}{D_0}\frac{p}{1-p}\left[1-\left(\frac{R_r}{R_m}\right)^{p-1}\right]$$

$$\times\left[1-\left(\frac{R_i}{r}\right)^{2p}\right]\left(\frac{r}{R_r}\right)^{p-1}\sin p\theta \quad (69)$$

$$D_0 = 2\left\{(1-\mu_r)\left(\frac{R_r}{R_m}\right)^{2p}+(1+\mu_r)\left(\frac{R_i}{R_m}\right)^{2p}\right.$$

$$\left. -\left[(1+\mu_r)+(1-\mu_r)\left(\frac{R_i}{R_r}\right)^{2p}\right]\right\}. \quad (70)$$

When $\mu_r = 1$, the equations are simplified to

$$B_{\text{III}r} = \frac{-B_r p}{1-p}\frac{1-\left(\frac{R_r}{R_m}\right)^{p-1}}{1-\left(\frac{R_i}{R_m}\right)^{2p}}\left[1+\left(\frac{R_i}{r}\right)^{2p}\right]$$

$$\times\left(\frac{r}{R_r}\right)^{p-1}\cos p\theta \quad (71)$$

$$B_{\text{III}\theta} = \frac{B_r p}{1-p}\frac{1-\left(\frac{R_r}{R_m}\right)^{p-1}}{1-\left(\frac{R_i}{R_m}\right)^{2p}}\left[1-\left(\frac{R_i}{r}\right)^{2p}\right]$$

$$\times\left(\frac{r}{R_r}\right)^{p-1}\sin p\theta. \quad (72)$$

b) Air-cored Halbach machine, i.e., $R_s \to \infty$

$$B_{\text{III}r} = \frac{4B_r}{D_0}\frac{p}{1-p}(1+\mu_r)\left[1-\left(\frac{R_r}{R_m}\right)^{p-1}\right]$$

$$\times\left[1+\left(\frac{R_i}{r}\right)^{2p}\right]\left(\frac{r}{R_r}\right)^{p-1}\cos p\theta \quad (73)$$

$$B_{\text{III}\theta} = \frac{-4B_r}{D_0}\frac{p}{1-p}(1+\mu_r)\left[1-\left(\frac{R_r}{R_m}\right)^{p-1}\right]$$

$$\times\left[1-\left(\frac{R_i}{r}\right)^{2p}\right]\left(\frac{r}{R_r}\right)^{p-1}\sin p\theta \quad (74)$$

$$D_0 = 2\left\{(1-\mu_r)\left[(1-\mu_r)\left(\frac{R_r}{R_m}\right)^{2p}+(1+\mu_r)\left(\frac{R_i}{R_m}\right)^{2p}\right]\right.$$

$$\left. -(1+\mu_r)\left[(1+\mu_r)+(1-\mu_r)\left(\frac{R_i}{R_r}\right)^{2p}\right]\right\}. \quad (75)$$

Again, when $\mu_r = 1$, the equations are simplified to

$$B_{\text{III}r} = \frac{-B_r p}{1-p}\left[1-\left(\frac{R_r}{R_m}\right)^{p-1}\right]\left[1+\left(\frac{R_i}{r}\right)^{2p}\right]$$

$$\times\left(\frac{r}{R_r}\right)^{p-1}\cos p\theta \quad (76)$$

$$B_{\text{III}\theta} = \frac{B_r p}{1-p}\left[1-\left(\frac{R_r}{R_m}\right)^{p-1}\right]\left[1-\left(\frac{R_i}{r}\right)^{2p}\right]$$

$$\times\left(\frac{r}{R_r}\right)^{p-1}\sin p\theta. \quad (77)$$

c) Halbach machine in air, i.e., $R_i \to 0, R_s \to \infty$

$$B_{\text{III}r} = -\frac{\frac{2B_r p}{1-p}(1+\mu_r)\left[1-\left(\frac{R_r}{R_m}\right)^{p-1}\right]\left(\frac{r}{R_r}\right)^{p-1}}{(1-\mu_r)^2\left(\frac{R_r}{R_m}\right)^{2p}-(1+\mu_r)^2}$$

$$\times\cos p\theta \quad (78)$$

$$B_{\text{III}\theta} = \frac{\frac{2B_r p}{1-p}(1+\mu_r)\left[1-\left(\frac{R_r}{R_m}\right)^{p-1}\right]\left(\frac{r}{R_r}\right)^{p-1}}{(1-\mu_r)^2\left(\frac{R_r}{R_m}\right)^{2p}-(1+\mu_r)^2}$$

$$\times\sin p\theta. \quad (79)$$

Further, when $\mu_r = 1$, the equations are simplified to

$$B_{\text{III}r} = B_r\frac{p}{1-p}\left[1-\left(\frac{R_r}{R_m}\right)^{p-1}\right]$$

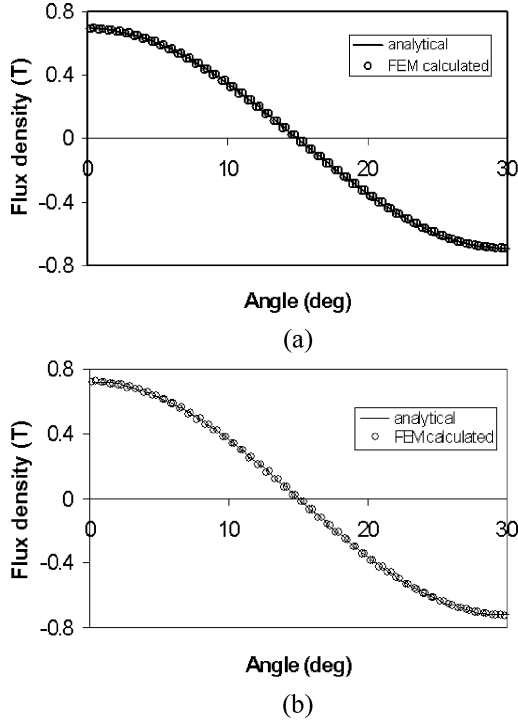$$\times\left(\frac{r}{R_r}\right)^{p-1}\cos p\theta \quad (80)$$

Fig. 2. Comparison of analytically and finite-element-predicted field distributions at $r = 27.4$ mm, for 12-pole, slotless, air-cored, internal rotor Halbach magnetized magnet machine with stator back iron. (a) $\mu_r = 1.3$. (b) $\mu_r = 1$.
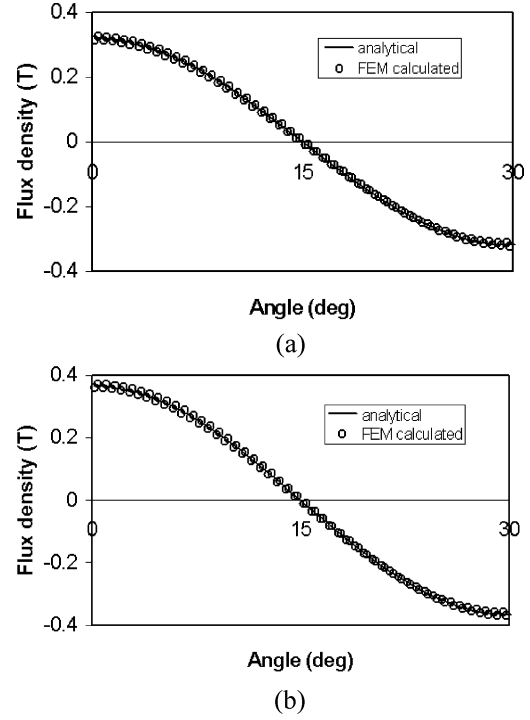

Fig. 3. Comparison of analytically and finite-element-predicted field distributions at $r = 27.4$ mm, for 12-pole, air-cored, Halbach magnetized ring magnet in air. (a) $\mu_r = 1.3$. (b) $\mu_r = 1$.

$$B_{\text{III}\theta} = -B_r \frac{p}{1-p} \left[1 - \left(\frac{R_r}{R_m} \right)^{p-1} \right]$$
$$\times \left(\frac{r}{R_r} \right)^{p-1} \sin p\theta. \tag{81}$$

The radial component of air-gap flux density in air-cored and iron-cored external rotor machines can also be expressed in the following unified form, viz.

$$B_{\text{air gap}} = B_{\text{III}r} = \frac{4B_r}{D_0} \frac{p}{1-p} \left[1 - \left(\frac{R_r}{R_m} \right)^{p-1} \right]$$
$$\times \left[1 + \left(\frac{R_i}{r} \right)^{2p} \right] \left(\frac{r}{R_r} \right)^{p-1} \cos p\theta \tag{82}$$

$$D_0 = 2 \left\{ K \left[(1-\mu_r) \left(\frac{R_r}{R_m} \right)^{2p} + (1+\mu_r) \left(\frac{R_i}{R_m} \right)^{2p} \right] \right.$$
$$\left. - \left[(1+\mu_r) + (1-\mu_r) \left(\frac{R_i}{R_r} \right)^{2p} \right] \right\} \tag{83}$$

where $K = 1$ and $(1-\mu_r)/(1+\mu_r)$, respectively, for iron-cored and air-cored external rotor machines, the same as was the case for internal rotor machines.

When $\mu_r = 1$, their ratio at the same radius can be expressed as

$$\frac{B_{\text{air gap}}(\text{air-cored})}{B_{\text{air gap}}(\text{iron-cored})} = 1 - \left(\frac{R_i}{R_m} \right)^{2p} \tag{84}$$

Clearly, it depends on the pole number and the ratio of R_i/R_m, or the ratio of R_r/R_m if the air-gap length $(R_r - R_i)$ is fixed.

IV. VALIDATION

Fig. 2(a) compares analytically and finite-element-predicted radial flux density distributions in the air gap (at $r = 27.4$ mm) of an air-cored internal rotor, slotless stator Halbach magnetized magnet machine, for which the remanence of the bonded anisotropic NeFeB magnet $= 0.655$ T, its relative recoil permeability $\mu_r = 1.3$, which corresponds to a $(BH)_{\text{max}}$ of 66 kJ/m^3, $R_r = 22.4$ mm, $R_m = 27$ mm, $R_s = 27.5$ mm. Fig. 2(b) compares predictions when μ_r is assumed to be equal to 1.0. Fig. 3 compares analytically and finite-element-calculated radial flux density distributions when the Halbach machine is in air, again for $\mu_r = 1$ and 1.3, while Fig. 4 shows the radial flux density distributions at $r = 21.5$ mm for an external rotor machine topology for $\mu_r = 1$ and 1.3, when $R_m = R_s = 27$ mm, $R_r = 22.4$ mm, and $R_i = 21.4$ mm. As can be seen, excellent agreement is achieved between analytical and finite-element predictions for both internal and external rotor machines. The influence of the relative recoil permeability on the field distribution is relatively small when the air gap is small. However, it becomes more significant when the air gap is increased, for example, when the magnet is placed in air.

Two 12-pole internal rotor demonstrator machines have been manufactured (Fig. 5). Both have identical unskewed stators, with 18 slots and a nonoverlapping winding. Both rotor ring magnets have an almost ideal Halbach magnetization. One rotor has an air-cored Halbach oriented and magnetized ring magnet rotor made from injection moulded bonded anisotropic NdFeB powder (Dai Nippon Ink & Chemicals' Compodic NDA502E) [6], while the second is iron-cored. However, its magnet thickness is thinner than that in the air-cored rotor such that it produces a similar air-gap field. The leading parameters for the
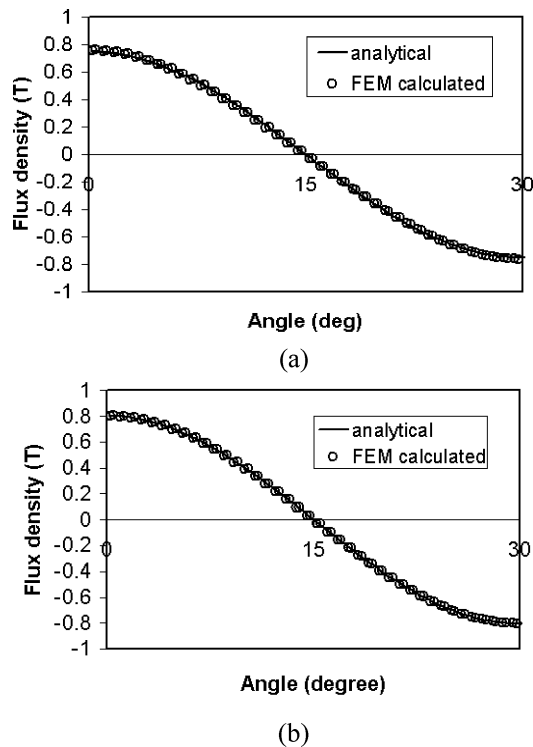
Fig. 4. Comparison of analytically and finite-element-predicted predicted field distributions at $r = 21.5$ mm, for 12-pole, slotless, iron-cored, external rotor Halbach magnetized magnet machine. (a) $\mu_r = 1.3$. (b) $\mu_r = 1$.
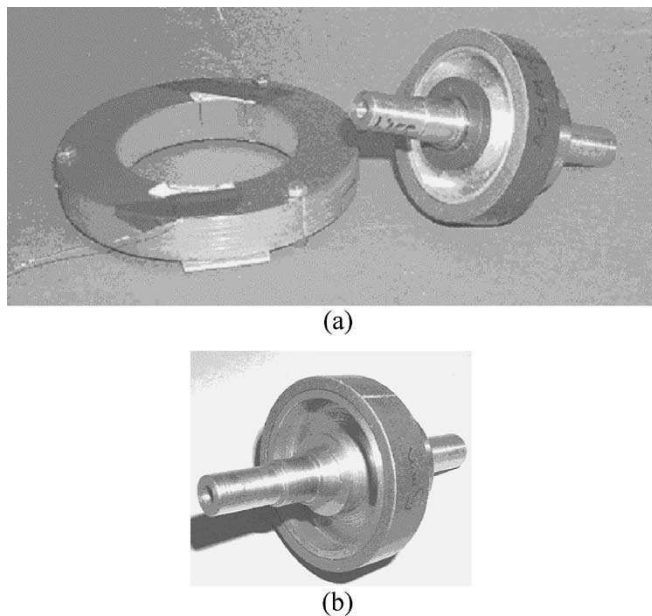

Fig. 5. 12-pole Halbach magnetized internal rotor used for air-gap field measurement. (a) Slotless laminated stator with search coils, and air-cored Halbach rotor. (b) Iron-cored Halbach rotor.

two machines are $B_r = 0.655$ T, $\mu_r = 1.3$, $R_s = 27.5$ mm, $R_m = 27$ mm, while $R_r = 22.4$ and 23.5 mm for the air-cored and iron-cored rotor machines, respectively. In order to measure the air-gap flux density distribution, a slotless laminated stator is employed and full pole-pitched search coils are used to measure the induced voltage, which is then integrated into obtain the air-gap flux density. Fig. 6 compares the measured and pre-
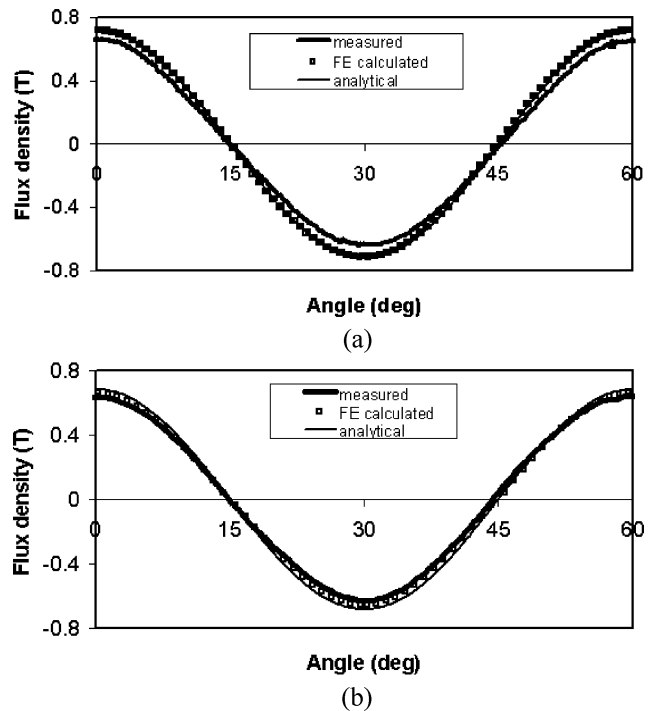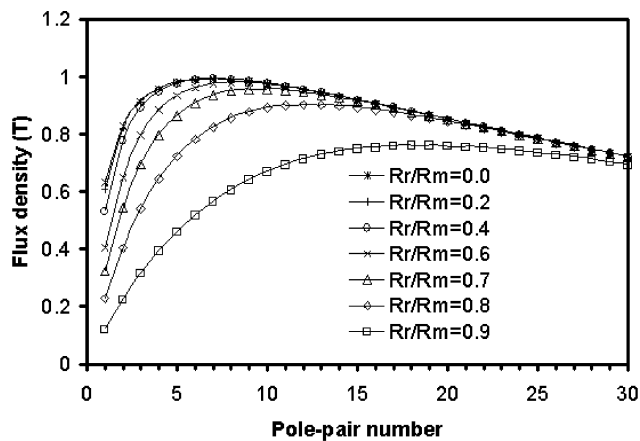

Fig. 6. Comparison of predicted and measured air-gap flux density distributions. (a) Air-cored rotor. (b) Iron-cored rotor.
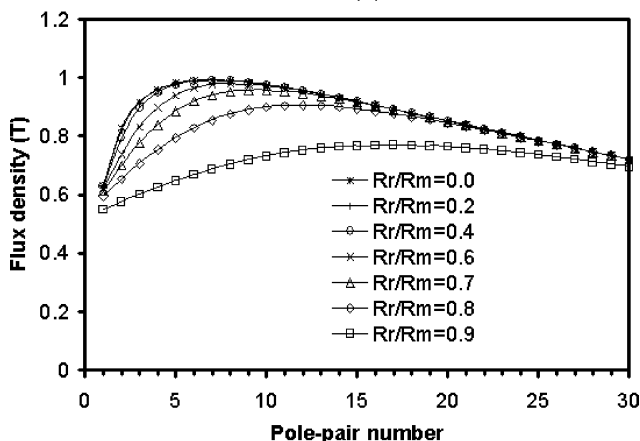
dicted air-gap field distributions. It can be seen that similar amplitudes of the air-gap flux density have been achieved for both air-cored and iron-cored machines although the magnet thicknesses are significantly different, and that their variation with respect to angular displacement are essentially sinusoidal. The measured results are slightly lower than the predicted values, which may be attributed in part to the magnet powder not being fully aligned and magnetized, as was observed in [7].

V. INVESTIGATION

Fig. 7 shows the variation of the calculated air-gap flux density (at $r = 27.4$ mm) for different magnet thicknesses (R_r/R_m) and numbers of pole pairs, for an internal rotor machine, for which $R_s = 27.5$ mm, $R_m = 27$ mm, $B_r = 0.655$ T, and $\mu_r = 1$. It can be seen that in contrast to conventional radial or parallel magnetized rotors, in which the length of the magnetic flux path in the magnets is constant (equal to the magnet thickness) and, hence, the peak air-gap flux density is almost independent of the pole number, both the effective cross-sectional area and the length of the flux paths in a Halbach magnetized magnet depend on the pole number, and consequently the peak air-gap flux density varies significantly with pole number. It can also be seen that for both air-cored and iron-cored rotor machines, an optimum combination for the number of pole pairs and the rotor magnet thickness exists for maximum air-gap flux density, as shown in Fig. 8. The thinner the magnet, the higher the optimum pole-pair number. In general, the optimum pole-pair number is higher for an air-cored rotor than for an equivalent iron-cored rotor. However, when the magnet thickness is increased, the difference diminishes. This is also reflected in Fig. 9, which shows the variation of the normalized air-gap flux density with the magnet thickness for

(a)

(b)

Fig. 7. Variation of peak air-gap flux density with pole-pair number for different magnet thicknesses. (a) Air-cored rotor. (b) Iron-cored rotor.
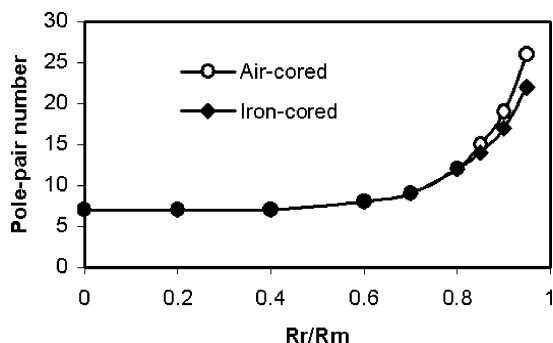

Fig. 8. Variation of optimum pole-pair number with rotor magnet thickness. ($R_s = 27.5$ mm, $R_m = 27$ mm).

both air-cored and iron-cored rotors. Since the electromagnetic torque is proportional to the rotor volume, the air-gap flux density and the electric loading, when the magnet thickness R_r/R_m is varied, while the stator bore radius R_s and the rotor outer radius R_m, as well as the current excitation are fixed, the torque varies in proportion to the air-gap flux density. Hence, the variation of the normalized torque is identical to that of the normalized air-gap flux density, as shown in Fig. 9. It can be seen that by employing rotor back iron the air-gap flux density, and, consequently, the electromagnetic torque, can be enhanced significantly compared to an air-cored rotor if the radial thick-
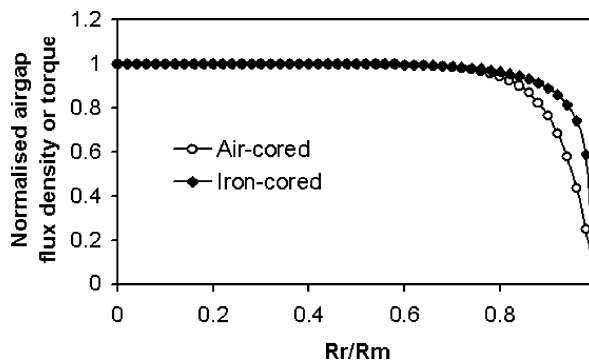

Fig. 9. Variation of normalized air-gap flux density and electromagnetic torque with rotor magnet thickness. ($R_s = 27.5$ mm, $R_m = 27$ mm).

ness of the magnet is small. Alternatively, the magnet thickness for an iron-cored rotor may be significantly less than for an air-cored rotor having the same torque capability and volume envelope.

VI. CONCLUSION

Analytical models, formulated in polar coordinates, have been developed for predicting the field distribution in Halbach magnetized permanent-magnet machines, accounting for the relative permeability of the magnets. They are general in nature and are therefore applicable to both internal and external rotor machines having either an iron-cored or air-cored stator and rotor. Since the developed models are analytically based and take significantly less computing time than the finite-element method, they are eminently suitable for use during the initial design of Halbach magnetized machines. Predicted results from the analytical models have been compared with finite-element predictions, and excellent agreement has been achieved. It has been shown that the air-gap flux density varies significantly with the pole number, and an optimal combination of magnet thickness and pole number exists for maximum flux density. It has also been shown that if the radial thickness of the magnet is relatively small, the air-gap field and electromagnetic torque can be enhanced by employing rotor back iron.

REFERENCES

[1] Z. Q. Zhu and D. Howe, "Halbach permanent magnet machines and applications—a review," *Proc. Inst. Elect. Eng.—Electric Power Applications*, vol. 148, no. 4, pp. 299–308, 2001.

[2] K. Halbach, "Design of permanent magnet multipole magnets with oriented rare earth cobalt material," *Nucl. Instrum. Methods*, vol. 169, pp. 1–10, 1980.

[3] M. Marinescu and N. Marinescu, "New concept of permanent magnet excitation for electrical machines—analytical and numerical computation," *IEEE Trans. Magn.*, vol. 28, pp. 1390–1393, Mar. 1992.

[4] J. Ofori-Tenkorang and J. H. Lang, "A comparative analysis of torque production in Halbach and conventional surface-mounted permanent magnet synchronous machines," in *Proc. IEEE Industry Applications Soc. Annu. General Meeting*, 1995, pp. 657–663.

[5] K. Atallah and D. Howe, "The application of Halbach cylinders to brushless ac servo motors," *IEEE Trans. Magn.*, vol. 34, pp. 2060–2062, July 1998.

[6] Z. Q. Zhu, Z. P. Xia, K. Atallah, G. W. Jewell, and D. Howe, "Powder alignment system for anisotropic bonded NdFeB Halbach machines," *IEEE Trans. Magn.*, vol. 36, pp. 3349–3352, Sept. 2000.

[7] ——, "Analysis of anisotropic bonded NdFeB Halbach machines accounting for partial powder alignment," *IEEE Trans. Magn.*, vol. 36, pp. 3575–3577, Sept. 2000.

Z.P. Xia received the B.Eng. and M.Sc. degrees from Zhejiang University, Hangzhou, China, in 1982 and 1985, respectively, and the Ph.D. degree from the University of Sheffield, Sheffield, U.K., in 2002, all in electrical and electronic engineering.

Since graduation, she has worked at Zhejiang University, China Institute of Metrology, The University of Sheffield, IMRA Europe S.A.S.—U.K. Research Center. Currently, she is a Research Associate at the University of Sheffield, working on the design and analysis of permanent-magnet brushless machines.

Z. Q. Zhu (M'90–SM'00) received the B.Eng. and M.Sc. degrees from Zhejiang University, Hangzhou, China, in 1981 and 1984, respectively, and the Ph.D. degree from the University of Sheffield, Sheffield, U.K., in 1991, all in electrical and electronic engineering.

From 1984 to 1988, he lectured in the Department of Electrical Engineering at Zhejiang University. Since 1988, he has been with the University of Sheffield, where he is currently Professor of Electrical Engineering. His current major research interests include applications, control, and design of permanent-magnet machines and drives.

David Howe received the B.Tech and M.Sc. degrees from the University of Bradford, Bradford, U.K., in 1966 and 1967, respectively, and the Ph.D. degree from the University of Southampton, Southampton, U.K., in 1974, all in electrical power engineering.

He has held academic posts at Brunel and Southampton universities, and spent a period in industry with NEI Parsons Ltd. working on electromagnetic problems related to turbo-generators. He is currently Professor of Electrical Engineering, Head of the Electrical Machines and Drives Research Group, and Director of the Rolls-Royce University Technology Centre in Advanced Electrical Machines and Drives at the University of Sheffield. His research activities span all facets of controlled electrical drive systems, with particular emphasis on permanent-magnet excited machines.

Prof. Howe is a Chartered Engineer, a Fellow of the Royal Academy of Engineering, and a Fellow of the IEE.